COBEM2003 - 1790 Copyright © 2003 by ABCM

Design of Aerodynamic Shapes by Means of Inverse Method

Quadros, R. S.; De Bortoli, A.L.
UFRGS, Graduate Program in Applied Mathematics - PPGMAp
Bento Gonçalves 9500, 91509-900, Fax:(051)3316-7301 - Porto Alegre - RS, Brazil
quadros@mat.ufrgs.br, dbortoli@mat.ufrgs.br

ABSTRACT: This work develops an efficient technique for modeling aerodynamic bodies submitted to flows at high speeds. The inverse method, based on the Elastic Membrane Technique, is used to find a new geometry. Pressure coefficient results from the Euler equations solved by the finite volume, explicit Runge-Kutta five-stages scheme. Numerical tests are carried out for NACA 0012, 0009 and a new geometry for Mach 0.8 using the Euler equations and the results are found to compare favorably with experimental or numerical data available in the literature. Besides, the technique build on earlier ones, because optimization shape coefficients are adequately evaluated.

keywords: *aerodynamics, optimization, inverse method, finite volume, Runge-Kutta.*

1. INTRODUCTION

Engineering field problems are defined by the governing differential or integral equations, shapes and size of the domains, boundary and initial conditions, material properties of the media, internal sources and external forces or inputs. If all of this information is known, the problem is of direct type and, generally, considered as well posed and solvable. If any of this information is unknown or unavailable, the problem becomes an indirect (or inverse) and is generally considered to be will posed and unsolvable.

The design of optimal aerodynamic shapes can be classified in two categories: the direct and the inverse. The first intends to find the best global aerodynamic property. Otherwise, the inverse form requires a local property, such as the Cp (pressure coefficient), of the final configuration satisfying the development objective. The optimization algorithm implemented here modifies the form of an airfoil until finding the improved form for data coefficient (Cp). The advantage of the finite volume implementation is that the flux is locally verified, in agreement with the idea of the inverse project for the attainment of the geometric form of a body.

The work mean objective is the attainment of a technique for the optimized modeling of bodies, such as an airfoil, submitted to transonic flows. The technique is developed using Fourier series for a set of two linear equations with proper boundary conditions, based on the Elastic Membrane Technique (Baker, 1999; Dulikravich & Baker, 1999).

Numerical tests are carried out for the NACA 0012, 0009 and a new profile, based on NACA profiles for Mach 0.8 using the Euler equations. These results showed to compare favorably with experimental data found in the literature and this method is being extended to find new aerodynamic shapes in an efficient manner. Following, the numerical procedure turns clear the numerical implementation.

2. GOVERNING EQUATIONS AND SOLUTION PROCEDURE

The governing equations for non viscous flows are the Euler equations in which mass, momentum and energy are conserved. They can be written for unsteady two-dimensional compressible flows in differential form as

$$\frac{\partial \vec{W}}{\partial t} + \frac{\partial \vec{F}_1}{\partial x} + \frac{\partial \vec{F}_2}{\partial y} = 0 \tag{1}$$

where

$$\vec{W} = \left\{ \begin{array}{c} \rho \\ \rho u \\ \rho v \\ \rho E \end{array} \right\}, \qquad \vec{\vec{F}} = \left\{ \begin{array}{c} \rho\vec{q} \\ \rho u\vec{q} + p.\vec{i} \\ \rho v\vec{q} + p.\vec{j} \\ \rho H\vec{q} \end{array} \right\}, \qquad \vec{\vec{F}} = \vec{F}_1\vec{i} + \vec{F}_2\vec{j}$$

and ρ is the fluid density, $\vec{q}$ the velocity vector ($\vec{q} = u\vec{i} + v\vec{j}$) and p the pressure.

Since the integral form of conservation laws allow discontinuities, the approach is suitable for capturing shocks in the flow field (kroll & Jain, 1987). The total energy E and enthalpy H are

$$E = e + \frac{u^2 + v^2}{2}, \qquad H = E + \frac{p}{\rho}$$

where e is the internal energy. To close this system of equations the state relation for a perfect gas is employed

$$p = \rho RT = (\gamma - 1)\rho(E - \frac{u^2 + v^2}{2}) \tag{2}$$

where R is the gas constant and γ the specific heat ratio. Eq.(1) can be cast into the integral form (Kroll & Jain, 1987)

$$\int_V \frac{\partial \vec{W}}{\partial t} dV + \int_S (\vec{\vec{F}}.\vec{n}) dS = 0 \tag{3}$$

One of the differences among the various finite volume formulations known in the literature is the arrangement of the control volume and update points for the flow variables (Kroll & Jain, 1987). The most frequently used schemes are the cell-centered, cell-vertex and node-centered approach. Each of these schemes has its own advantages and disadvantages (De Bortoli, 2002). The discretization used is based on the node-centered arrangement, as shown in figure 1.

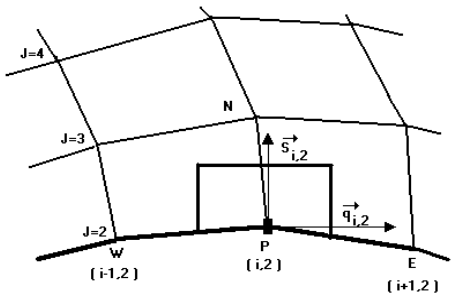

Figure 1: Node-centered arrangement

In the computational domain the cell vertices are identified by their indices (i,j). As Eq. 1 is valid for arbitrary control volume, it is also valid for $V_{i,j}$ that means

$$\frac{\partial \vec{W}_{i,j}}{\partial t} = -\frac{1}{V_{i,j}} \int_S (\vec{\vec{F}}.\vec{n}) dS \tag{4}$$

The finite volume discretization based on the central averaging is not dissipative. The numerical procedure does not converge to the steady state when the high frequency oscillations of error in the solution are not damped. To avoid these oscillations dissipative terms are introduced. The optimum amount of artificial viscosity is mainly determined by the smoothing properties of relaxation and is written as follows (Kroll & Jain, 1987)

$$\frac{\partial W_{i,j}}{\partial t} + \frac{1}{V_{i,j}} [Q_{i,j} - D_{i,j}] = 0 \tag{5}$$

This dissipation operator is a blend of second and fourth differences and is defined according to

$$D_{i,j} = d_{i,j+1/2} - d_{i,j-1/2} + d_{i+1/2,j} - d_{i-1/2,j} \tag{6}$$

whose dissipation and other details are shown in the literature (Kroll & Jain, 1987; De Bortoli, 2002).

2.1 Optimization

The optimization of aerodynamic geometries can be classified in two categories: the direct and the inverse. The inverse form requires a local property, pressure coefficient in our case, of the final configuration satisfying the objectives of development. There are two classes of tools for inverse aerodynamic shape design: methods with coupled and with uncoupled shape changes and flow-field analysis.

The first requires special considerations when writing the flow-field computer code. These software modifications represent a major undertaking, even if the source version of the flow-field analysis code is available. The uncoupled inverse design tool requires no modification to an existing flow-field analysis code (a panel, an Euler or a Navier-Stokes code) and can be used in the uncoupled aerodynamic shape inverse design without need of alterations. The Elastic Membrane Technique is one example (Dulikravich, 1995).

For a given form of an airfoil, such as the NACA 0012, it is desired to find a new shape for a given coefficient. The advantage of the finite volume implementation here is that the flux is locally verified, in agreement with the idea of the inverse design technique for the attainment of the body geometry.

To the shape evolution, in the model used, one separates the upper and lower sides of the airfoil (Dulikravich, 1995; Dulikravich & Baker, 1999). On the upper side the Fourier series result

$$-\alpha_0 \Delta y^{top} + \alpha_1 \frac{d\Delta y^{top}}{ds} + \alpha_2 \frac{d^2 \Delta y^{top}}{d^2 s} = \Delta C_p^{top} \tag{7}$$

and on the lower airfoil contour

$$\alpha_0 \Delta y^{bot} + \alpha_1 \frac{d\Delta y^{bot}}{ds} - \alpha_2 \frac{d^2 \Delta y^{bot}}{d^2 s} = \Delta C_p^{bot} \tag{8}$$

where s is the airfoil contour coordinate, $\Delta Cp^{top,bot}$ the pressure coefficient difference between the desired and that at actual iteration and the α_i's are user constants, which control the rate of convergence of the shape evolution process.

The ΔCp in equations (7) and (8) can be represented using the Fourier series expansion of the form

$$\Delta C_p^{top,bot} = a_0 + \sum_{n=1}^{n_{max}} [a_n cos(N_n s) + b_n sin(N_n s)] \tag{9}$$

where $N_n = \frac{2\pi n}{L}$ and L is the total length of the airfoil contour.

The particular solution of either Eq. (7) and (8) can be represented in the general Fourier series form

$$\Delta y_p{}^{top,bot} = A_0 + \sum_{n=1}^{n_{max}} [A_n cos(N_n s) + B_n sin(N_n s)] \tag{10}$$

Since the Fourier coefficient of the particular solutions on the upper and lower airfoil contours are different, it can be expected that gaps will form at the leading and trailing edges of the airfoil. These gaps can be closed with appropriate homogeneous solutions to Eqs. (7) and (8). The upper contour homogeneous solution is

$$\Delta y_h^{top} = F^{top} e^{\lambda_1 s} + G^{top} e^{\lambda_2 s} \tag{11}$$

where

$$\lambda_{1,2} = \frac{\alpha_1 \pm \sqrt{\alpha_1{}^2 + 4\alpha_0 \alpha_2}}{2\alpha_2} \tag{12}$$

and F and G are as yet undetermined coefficients. Likewise, on the lower airfoil contour, the homogeneous solutions is

$$\Delta y_h^{bot} = F^{bot} e^{-\lambda_1 s} + G^{bot} e^{-\lambda_2 s} \tag{13}$$

Thus, the overall displacement of the airfoil contour is given by the following equations:

$$\Delta y_h^{top} = F^{top} e^{\lambda_1 s} + G^{top} e^{\lambda_2 s} + \sum_{n=1}^{n_{max}} [A_n^{top} cos(N_n s) + B_n^{top} sin(N_n s)] \tag{14}$$

$$\Delta y_h^{bot} = F^{bot} e^{-\lambda_1 s} + G^{bot} e^{-\lambda_2 s} + \sum_{n=1}^{n_{max}} [A_n^{bot} cos(N_n s) + B_n^{bot} sin(N_n s)] \tag{15}$$

The four unknown constants F and G can now be determined for the upper and lower airfoil contours such that the following four boundary conditions are met:

- for trailing edge displacement, $\Delta y^{bot}(0) = 0$;
- for trailing edge closure, $\Delta y^{bot}(0) = \Delta y^{top}(L)$;
- for leading edge closure, $\Delta y^{bot}(S_{Le}) = \Delta y^{top}(S_{Le})$ and
- for smooth leading edge deformation, $\frac{d}{ds}\Delta y^{bot}(S_{Le}) = \frac{d}{ds}\Delta y^{top}(S_{Le})$,

where Δy is the variation in the y-direction, L the total lenght and S_{Le} is the value of the contour at the leading edge.

The two-dimensional Fourier series shape evolution equation can be expanded to three dimensions, using the same idea to k-planes as in the two-dimensional case (De Bortoli and Quadros, 2003).

3. NUMERICAL RESULTS

In the following, numerical results for NACA 0012 and 0009 airfoils and a new form based on them are presented. The calculations have been carried out on a O-type grid which consists of 192x60 cells, as shown in figure 2; it is refined in the direction next the surface of the body (airfoil contour), where the flow variables will have the biggest gradients. The position of the outer boundary is around thirty chord lengths away from the airfoil.

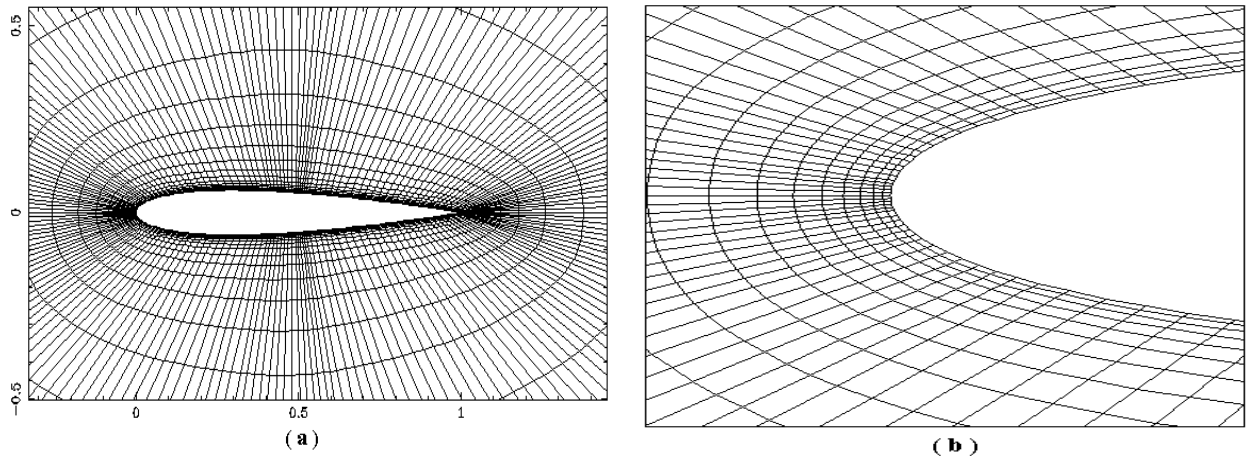

Figure 2: Structured O-type grid for NACA 0012 (a) and leading edge amplification (b), 192x60 cells.

The pressure lines for NACA 0012, NACA 0009 and new airfoil (without shock) for Mach = 0.8 and $\alpha = 0^o$ is shown in figure 3 (a, b and c). One notices that our code capture very well the shocks over both airfoils. The

pressure coefficient for NACA 0012 and a new profile over these geometries is shown in figure 3d. The airfoil shape obtained, after twenty iterations using the Fourier series technique, develops a shock at approximately 50% chord/length relation for NACA 0012 airfoil and disappears for the thinner profile.

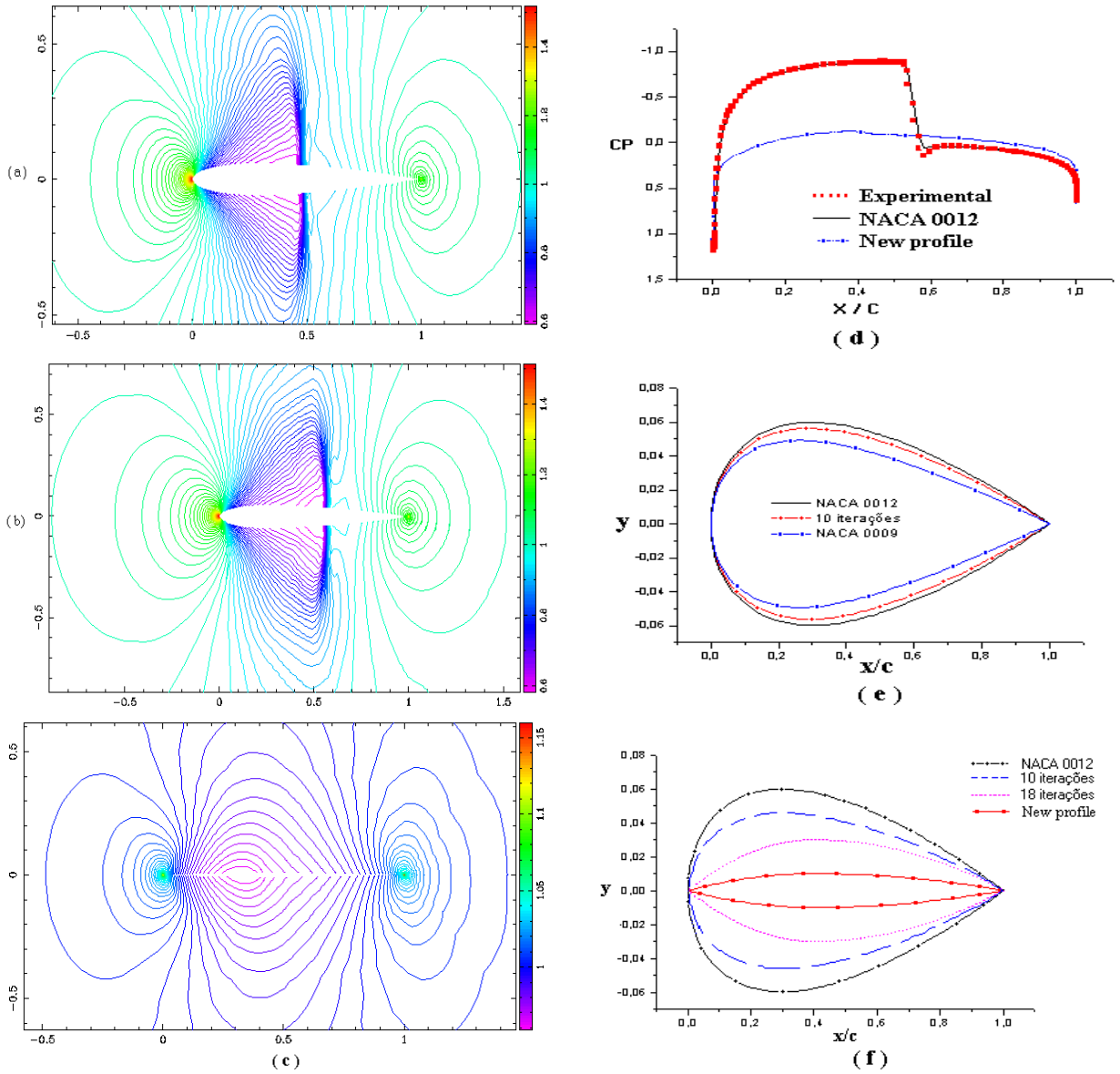

Figure 3: Pressure lines for: (a) NACA 0012, (b) NACA 0009, (c) new profile, and (d)corresponding pressure coefficient; geometry evolution using the inverse method finding: (e) NACA 0009 and (f) new profile, respectively, for Mach = 0.8 and $\alpha = 0^o$.

To check the accuracy of the method, results for the NACA 0012 airfoil are compared to a solution obtained by the conformal mapping technique for incompressible flow (Blazek, 1994) and with experiments for compressible flows (Kroll & Jain, 1987).

Figures 3 *e* and *f* show the geometry evolution. Starting with the NACA 0012 airfoil, after 25 iterations the NACA 0009 shape is obtained, using the inverse method for parameters $\alpha_0 = 1.2$, $\alpha_1 = 0.0$ and $\alpha_2 = 0.4$, which were obtained solving a system. Otherwise, starting the process with the NACA 0012 , after 25 iterations other profile can be obtained for specified pressure coefficient.

Finally, the comparison of the rate of convergence of the form evolution for two sets of parameters is

presented in the figure 4. Parameters $\alpha_0 = 0{,}4$, $\alpha_1 = 0{,}0$ and $\alpha_2 = 1{,}2$ presented less oscillations during the geometry evolution, being the most indicated in the attainment of the results presented here.

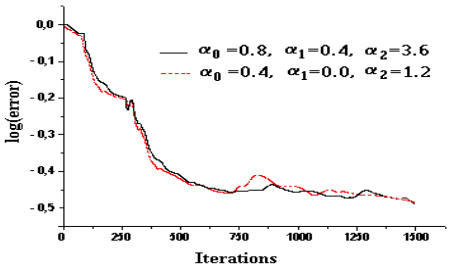

Figure 4: Shape evolution convergence rate comparison for different parameters used for the inverse method.

4. CONCLUSIONS

The inverse shape design, based on the Elastic Membrane Technique, using Fourier Series (Baker, 1999), showed to be efficient finding new aerodynamic geometries for given pressure coefficient differences. This method does not require modification of the flow analysis software and converges fast for transonic flows.

The method showed to be efficient finding not only the pressure coefficient for aerodynamic geometries, but also in the determination of a new geometry for a given pressure coefficient, even when the geometry is almost a flat plate at zero degrees inclination to the mean flow stream. Such is done with around 25 iterations, when using the appropriate Fourier series coefficients. Besides, this method can be extended to three-dimensional situations, as wings (formed from a number of airfoils) or other complex geometries.

It is the author's opinion that the comparison between experimental and numerical results is encouraging; therefore, the present technique is being extended for solving three-dimensional flows over aerodynamic geometries as wings and complete airplanes.

References

[1] Baker, D.P., 1999. A Fourier Series Approach to the Elastic Membrane Inverse Shape Design Problem in Aerodynamics, Master's thesis, Dept. of Aerospace Eng. - Pennsylvania State University.

[2] Blazek, J., 1994. Verfahren zur Beschleunigung der Lösung der Euler - und Navier-Stokes Gleichungen bei Stationären Über - und Hyperschallströmungen, Ph. D Thesis, University of Braunschweig.

[3] De Bortoli, A. L., 2002. Multigrid Based Aerodynamical Simulations for the NACA 0012 Airfoil, *Applied Numerical Mathematics 20*, pp 337-349.

[4] De Bortoli, A. L., Quadros, R. S., 2003. Euler Solution for Aerodynamic Inverse Shape Design, Submitted to Int. J. for Num. Meth. in Fluids.

[5] Dulikravich, G.S., 1995. Shape Inverse Design and Optimization for Three Dimensional Aerodynamics, *AIAA paper 95-0695, Reno, Nevada - USA.*

[6] Dulikravich, G.S., Baker, D.P., 1999. Aerodynamic Shape Inverse Design Using a Fourier Series Method, *AIAA paper 99-0185.*

[7] Kroll, N., Jain, R. K., 1987. Solution of two-dimensional Euler Equations - Experience with a Finite Volume Code, Forschungsbericht, DFVLR-FB 87-41.